June 30, 1997

Unified QCD Description of Hadron and Jet Multiplicities in e^+e^- Annihilation.

Sergio Lupia* and Wolfgang Ochs†

Max-Planck-Institut für Physik, (Werner-Heisenberg-Institut)
Föhringer Ring 6, 80805 München, Germany

Abstract

The evolution equation for parton multiplicities in quark and gluon jets which takes into account the soft gluon interference is solved numerically using the initial conditions at threshold. If the $k_\perp$-cutoff Q_c is lowered towards the hadronic scale Q_0 of a few hundred MeV the transition from the jet multiplicity to the hadron multiplicity is well described with a common normalization. Evidence is presented within this approach that the coupling $\alpha_s(Q^2)$ rises by more than a factor of 10 when approaching the low energy region. The ratio of hadron multiplicities in gluon and quark jets is found smaller than in previous approximate solutions of the evolution equation.

Paper submitted to the XVIII Int. Symp. on Lepton-Photon Interactions, Hamburg, Germany, 28 July - 1 August 1997

*E-mail address: lupia@mppmu.mpg.de
†E-mail address: wwo@mppmu.mpg.de

1 Introduction

One of the simplest characteristics of the hadronic final state is the particle multiplicity. Following the ideas of a soft confinement mechanism [1,2] the observable mean hadron multiplicity in a quark or gluon jet is expected to follow closely the multiplicity of the final QCD partons in its energy dependence. More specifically, within the picture of local parton hadron duality (LPHD) [3] the primary parton of energy E generates a parton cascade which is evolved down to small scales with a transverse momentum cutoff Q_0 of a few hundred MeV. Then, within the so-called modified leading logarithmic approximation (MLLA), which takes into account the leading double logarithmic and next to leading single logarithmic terms, a good description of the mean charged particle multiplicity in $e^+e^- \to$ hadrons as a function of the primary *cms* energy $\sqrt{s} \equiv Q = 2E$ is obtained with a formula

$$\mathcal{N}_{ch}(Q) = 2K_{ch}\mathcal{N}_q(\frac{Q}{Q_0}, \frac{Q_0}{\Lambda}) + \text{const.} \tag{1}$$

Here $\mathcal{N}_q$ denotes the multiplicity of partons in a single quark jet of energy E and Λ is the QCD scale for the coupling constant. From fits in the energy range $Q = 3 \ldots 160$ GeV one typically finds $Q_0 \gtrsim \Lambda \approx 250$ MeV and the normalization $K_{ch} \approx 1.2$ [3–5]. Assuming $K_{ch} = \frac{2}{3}K_{all}$ the number of all final state hadrons (charged and neutral) is then about twice as large as the number of partons ($K_{all} \approx 2$).

Another characteristic of the final state is the mean multiplicity of jets $\mathcal{N}(Q, Q_c)$ for a given resolution parameter Q_c, or, in conventional normalization, $y_c = \frac{Q_c^2}{Q^2}$. Early results at low resolution (large y_c) in $\mathcal{O}(\alpha_s^2)$ [6] played an important role as QCD test and in the determination of the running coupling constant α_s. The calculation of jet multiplicities to all orders in α_s became feasible using the Durham/$k_\perp$ algorithm [7] which takes as separation parameter for two jets the measure

$$y_{ij} = 2 \min\,(E_i^2, E_j^2)\, \frac{1 - \cos\Theta_{ij}}{Q^2} \tag{2}$$

which for small relative angles Θ_{ij} approximates the rescaled transverse momentum $(k_\perp^{ij})^2/Q^2$ of the jet of lower momentum with respect to the one of higher momentum. Then the jet multiplicity $\mathcal{N}_{jet}(y_c, Q)$ refers to all jets with separation $y_{ij} \geq y_c$. Jet multiplicities in leading and next-to-leading order of $\ln y_c$ have been calculated [8–10] and, after matching with the full $O(\alpha_s)$ results, a good description of jet multiplicities down to $y_c \sim 10^{-3} \ldots 10^{-4}$ has been obtained [11,12]. In these calculations the jet multiplicities are given in absolute normalization ($K_{all}=1$) by

$$\mathcal{N}(Q,Q_c) = 2\mathcal{N}_q(\frac{Q}{Q_c},\frac{Q_c}{\Lambda}). \tag{3}$$

In this paper we investigate whether both phenomena, jet multiplicities and hadron multiplicities, can be described in a unified way. Indeed, the resummation of the perturbative series has been achieved in both cases by using the same type of evolution equation. Also, the Durham/$k_\perp$ algorithm of the jet definition (2) coincides for $Q_c \to Q_0$ with the prescription $k_\perp \geq Q_0$ which is applied in the description of hadrons within the LPHD picture. At first sight there is no smooth transition for $Q_c \to Q_0$ from (3) to (1) because of the additional constants in (1). Furthermore, various jet observables for small y_c deviate from the perturbative predictions (see, for example, review [13]), and this is often taken as evidence for nonperturbative hadronization effects at resolution scales $Q_c \sim 1-2$ GeV.

We will show that these problems – in the case of the mean jet or particle multiplicity – disappear if the underlying coupled evolution equations for quark and gluon jets are solved with sufficiently high accuracy, here we perform a numerical integration to obtain the exact solutions. An important role is played by the running coupling constant which leads to a maximal relative separation of particle and jet multiplicities ($\mathcal{N}-2$) near threshold $y_c \to 1$.

2 Evolution equation for multiplicities

We start from the evolution equation for the generating functional of the multiparton final state [14,15] which, in the parton splitting process $A \to BC$, takes into account angular ordering [16], energy conservation and the running coupling at one loop order. By appropriate differentiation we obtain the evolution equations for the mean parton multiplicities $\mathcal{N}_q$ and $\mathcal{N}_g$ in quark and gluon jets with jet virtuality κ (see also [10]) or with

$$\eta = \ln\frac{\kappa}{Q_c}, \qquad \kappa = Q\sin\frac{\Theta}{2}. \tag{4}$$

where Θ denotes the maximum angle between the outgoing partons B and C. At fixed cutoff Q_c these equations read

$$\begin{aligned}
\frac{d\mathcal{N}_g(\eta)}{d\eta} &= \int_{z_c}^{1-z_c} dz\frac{\alpha_s(k_\perp^2)}{2\pi}[\Phi_{gg}^{asy}(z)\{\mathcal{N}_g(\eta+\ln z)+\mathcal{N}_g(\eta+\ln(1-z))-\mathcal{N}_g(\eta)\} \\
&\quad +n_f\Phi_{gq}(z)\{\mathcal{N}_q(\eta+\ln z)+\mathcal{N}_q(\eta+\ln(1-z))-\mathcal{N}_g(\eta)\}] \qquad (5)\\
\frac{d\mathcal{N}_q(\eta)}{d\eta} &= \int_{z_c}^{1-z_c} dz\frac{\alpha_s(k_\perp^2)}{2\pi}\Phi_{qg}(z)\{\mathcal{N}_g(\eta+\ln z)+\mathcal{N}_q(\eta+\ln(1-z))-\mathcal{N}_q(\eta)\}.
\end{aligned}$$

The boundaries of the integral over the parton momentum fractions z are determined by the lower cutoff in the transverse momentum measure $\tilde{k}_\perp$ defined according to (2) with the approximation $z_A \approx 1 - z_B$

$$\tilde{k}_\perp = \min(z, 1-z)\kappa \;\geq\; Q_c. \tag{6}$$

The lower bound z_c in (5) is obtained for minimal $z = Q_c/(Q \sin\frac{\Theta}{2})$ which is found for $\Theta \approx \frac{\pi}{2}$ (in this configuration, because of transverse momentum conservation, the high energy secondary parton has production angle $\vartheta_A \approx 0$ and the soft particle $\vartheta_B \lesssim \frac{\pi}{2}$); more generally, Θ corresponds to the half opening angle of the jet. Therefore z_c is given by

$$z_c = \frac{Q_c\sqrt{2}}{Q} = \sqrt{2y_c} = e^{-\eta}. \tag{7}$$

Since $z_c \leq \frac{1}{2}$, one finds $y_c \leq \frac{1}{8}$ and $\eta \geq \ln 2$.

The coupling is given by $\alpha_s(\tilde{k}_\perp, n_f) = 2\pi/(b\ln(\tilde{k}_\perp/\Lambda))$ with $b = (11N_C - 2n_f)/3$. We evolve $\alpha_s(\tilde{k}_\perp, n_f)^{-1}$ with $\tilde{k}_\perp$ by matching smoothly the couplings for n_f and $n_f + 1$ at the heavy quark thresholds. The splitting functions Φ_{AB} for parton splitting $A \to B$ are given by[17]

$$\begin{aligned}
\Phi_{qg}(z) &= \Phi_{qq}(1-z) = 2C_F\frac{1+(1-z)^2}{z}, & (8)\\
\Phi_{gq}(z) &= \Phi_{gq}(1-z) = 2T_R[z^2 + (1-z)^2], & (9)\\
\Phi_{gg}(z) &= \Phi_{gg}(1-z) = 4N_C\left[z(1-z) + \frac{1-z}{z} + \frac{z}{1-z}\right]. & (10)
\end{aligned}$$

with $N_C = 3$, $C_F = \frac{4}{3}$ and $T_R = \frac{1}{2}$. Because of its symmetry property it is convenient to replace $\frac{1}{2}\Phi_{gg}(z)$ by the asymmetric function $\Phi_{gg}^{asy}(z) = (1-z)\Phi_{gg}(z)$ in (5) [10].

The differential equations are defined only for $\eta \geq \ln 2$. The initial conditions for the solutions of (5) then read (for any fixed Q_c)

$$\mathcal{N}_g(\eta) = \mathcal{N}_q(\eta) = 1 \qquad \text{for} \quad 0 \leq \eta \leq \ln 2. \tag{11}$$

The evolution equations yield the complete leading and next-to-leading terms in the high energy expansion in $\sqrt{\alpha_s}$, the higher order terms allow the fulfilment of the boundary conditions at threshold. Such results in absolute normalization have been derived within the MLLA for gluon jets[18] and for the coupled system of quark and gluon jets[9]. Whereas the MLLA improves on the high energy behaviour, it leads to inconsistencies ($\mathcal{N}_a'(\eta) < 0$)

near threshold. In the present analysis we solve the equations (5) and (11) numerically.[1]

The two jets in e^+e^- annihilation evolve independently in this approximation. Near threshold this factorization of the generating functional does not hold any more and non-logarithmic terms become important. For the $k_\perp$ resolution criterion (2) the inelastic threshold is found for symmetric 3-jet events ($\Theta = \frac{2\pi}{3}$, $z = \frac{2}{3}$) with $y_c = \frac{1}{3}$ or $\eta = \frac{1}{2}\ln 3$. This is to be compared with $y_c = \frac{1}{8}$ and $\eta = \ln 2$ for eq. (5). The difference of thresholds will clearly affect the results in the large y_c region.

An improvement in this region can be achieved by replacing the contribution of $\mathcal{O}(\alpha_s)$ in (5) by the explicit result for $e^+e^- \to 3$ partons in $\mathcal{O}(\alpha_s)$ (see also Ref. [9,19]). The lowest order contribution $\mathcal{N}_q^{(1)}$ of the evolution equation is obtained by taking the first iteration of (5) with the initial conditions (11), i.e. replacing the three $\mathcal{N}$-terms in the curly brackets in (5) by unity. The full $\mathcal{O}(\alpha_s)$ contribution is then found by numerical integration of

$$\mathcal{N}^{3-jet}(y_c) = 2\int_{1/2}^{1} dx_1 \int_{1-x_1}^{x_1} dx_2 \Theta(d_{23} - y_c) \frac{C_F \alpha_s(\tilde{k}_\perp)}{2\pi} \frac{x_1^2 + x_2^2}{(1-x_1)(1-x_2)} \tag{12}$$

$$d_{23} = \min\left(\frac{x_2}{x_3}, \frac{x_3}{x_2}\right)(1-x_1) > y_c \tag{13}$$

where x_1 (x_2) denote the quark (antiquark) momentum fraction and $x_3 = 2 - x_1 - x_2$ the gluon momentum fraction. Here the coupling is taken again as running with the $k_\perp$ measure (2) $\tilde{k}_\perp = (d_{23}Q^2)^{\frac{1}{2}}$ as scale in the integration region $x_2 < x_1$ in (12). The $\mathcal{O}(\alpha_s)$ corrected solution $\mathcal{N}_{corr}^{e^+e^-}$ is then obtained from

$$\mathcal{N}_{corr}^{e^+e^-}(y_c) = 2N_q(y_c) - 2N_q^{(1)}(y_c) + \mathcal{N}^{3-jet}(y_c). \tag{14}$$

A corresponding improved result for the gluon jet is not yet available and has to be considered for each process separately.

In the present application we apply the equation (14) to the full range of scale parameters

$$Q_0 < Q_c < Q \quad \text{or} \quad \frac{Q_0}{Q} \le \sqrt{y_c} \le 1, \tag{15}$$

i.e. we study the jet region ($y_c \gtrsim 0.01$) and also the transition from the jets to the fully resolved hadrons ($y_c \sim (Q_0/Q)^2$).

[1]We start from $\mathcal{N}_a(\eta = \ln 2) = 1$, calculate $\mathcal{N}_a(\eta + \delta\eta)$ in steps of length $\delta\eta$ from the derivatives (5) as $\mathcal{N}_a'(\eta)\delta\eta$ using the trapezoidal rule for the integral and linear interpolation for the required $\mathcal{N}$ values under the integral. The integral is performed with logarithmic variable $y = \ln z$.

3 Comparison of predictions with experimental data.

3.1 Multiplicities in e^+e^- annihilation

In Fig. 1a we show the data of the average jet multiplicity [11,12] as a function of the resolution parameter $y_c = \frac{Q_c^2}{Q^2}$ as obtained with the $k_\perp$ algorithm. The theoretical predictions from (14) for the jet data are given in absolute normalization in terms of the single parameter Λ. Also shown are the data on hadron multiplicities [20] taken as $\mathcal{N}_{all} = \frac{3}{2}\mathcal{N}_{ch}$ as a function of the same scale parameter, now calculated as $y_c = \frac{Q_0^2}{Q^2}$ where Q_0 corresponds to the parton $k_\perp$ cutoff characterizing a hadronic scale according to the LPHD picture and is obtained from a fit to the data. Another adjustable parameter here is the overall normalization K_{all} which relates the parton and hadron multiplicities in $\mathcal{N}_{all} = K_{all} 2\mathcal{N}_q$. We determine first the Λ parameter from the jet multiplicity (lower data set in Fig. 1) and then the K_{all} and Q_0 from the hadronic multiplicity (upper data set). A good description of the data is obtained with parameters

$$K_{all} = 1, \qquad \Lambda = 500 \pm 50 \text{ MeV} \qquad \lambda = \ln \frac{Q_0}{\Lambda} = 0.015 \pm 0.005 \tag{16}$$

which correspond to the curves shown in Fig. 1a. The quantity $\mathcal{N} - 2$ derived from the same experimental data is shown in Fig. 1b. The dashed curves represent the contribution $2\mathcal{N}_q$ in (14) from the evolution equation alone. The fits can be seen to describe quantitatively the hadron multiplicity, the jet multiplicity for the small and large y_c, whereas in the intermediate region around $y_c \simeq 0.01$ the fit exceeds the data on $\mathcal{N} - 2$ by up to 20% (up to 5% in $\mathcal{N}$). Deviations of this type may indicate the importance of two-loop $\mathcal{O}(\alpha_s^2)$ terms not included in the analysis.

As a remarkable result of our analysis we find that the common normalization $K_{all} = 1$ is possible without difficulty; the normalization parameter K_{all} is correlated with Q_0 and can be varied within about 30%. The solution with $K_{all} = 1$ is natural as it provides the correct boundary conditions $\mathcal{N} = 2$ at threshold for both hadrons and jets. Then a continuous connection between jet and hadron data results and both are described by the same evolution equation (14). In this description a single hadron corresponds to a single parton of low virtuality Q_0.

Previous approximate solutions had been restricted to $y_c \gtrsim 0.002$ for jets, whereas for hadrons the analytical results could only be applied to the higher energy region with a larger K_{ch} factor.[2]

Our results are consistent with the previous determination from the energy moments [5] which also implied that that Q_0 should exceed Λ by not more than about 10%. On the other hand, the exact solution does not allow $Q_0 = \Lambda$ as the multiplicity would diverge in this case. This can be seen from the first iteration of (5), (the "Born-term"), which would give the contribution $\int_0^\eta dy/(y+\lambda)$. The lower curve in Fig. 1 reflects this singularity in the steep rise towards small y_c; it approaches the singularity at $y_\Lambda = \Lambda^2/Q^2$ but stops at the hadronization scale $y_0 = (Q_0)^2/Q^2 \gtrsim y_\Lambda$.

It is interesting to compare the two sets of data at the same y_c. The difference between the two curves comes entirely from the running of α_s. Namely, if α_s were kept fixed in equations (5) the resulting multiplicities would depend only on the ratio of the available scales through the variable $\eta = \ln\frac{\kappa}{Q_c} = -\frac{1}{2}\ln(2y_c)$ but not on the absolute size of Q_c and the two curves in Fig. 1 would coincide. A model with fixed α_s would predict at high energy a power like dependence on Q, i.e. a straight line in Fig. 1a between the two curves shown.

The splitting of the two curves and data sets in Fig. 1 is possible because of the introduction of the new scale Λ and comes entirely from the different values of $\alpha_s(\tilde{k}_\perp/\Lambda)$ in both cases. The largest difference occurs near the inelastic threshold at $y_c \approx \frac{1}{8}$ or $\eta \approx \ln 2$. In this region $\mathcal{N} - 2$ is dominated by the 3-jet production of order α_s and the jet and hadron results at the same y_c are in the ratio of the relevant typical coupling constants. At the lowest available data point for the hadron multiplicity ($Q = 3$ GeV) this ratio of couplings is greater than 10, so the typical coupling to produce hadrons at 3 GeV is $\alpha_s \gtrsim 1$. The good matching of the prediction for hadrons with the boundary condition at threshold suggests that the coupling is rising even more towards lower energies.

Similarly for the jet data, if we increase the resolution (lower y_c) the multiplicity is first rising very slowly because of the small coupling ($\alpha_s \sim 0.1$); for very high resolution, if Q_c is lowered from 900 MeV ($y_c \sim 10^{-4}$) to the final 500 MeV about three quarters of the final multiplicity are produced because of the strongly increasing coupling, three times as many jets as in the large complementary kinematic region. This behaviour is qualitatively described by the high energy DLA result $\mathcal{N} \sim K_0(A\sqrt{\lambda})I_1(A\sqrt{\ln(\kappa/\Lambda)}) + \ldots$

[2]The different value of the normalization factor as compared to previous analyses (for example [3–5]) is due to the use in the MLLA approximation of the initial conditions which have negative slope $\mathcal{N}'(\eta = 0) < 0$ and therefore lead to a delayed rise with energy [9]. Our exact solution in the present *cms* energy range is about twice as large and rises more slowly than the analytical MLLA solution for $Q_0 = \Lambda$ [18].

with $A = \sqrt{16N_C/b}$ which exhibits the logarithmic singularity $\sim 1/\ln\lambda$ for $Q_c \to \Lambda$.

It will be interesting to study this behaviour further near the transition $Q_c \to Q_0$, especially for the jet rates which vary strongly in the low y_c range. Note that the jet rates should be calculated from all final state hadrons, not only from the charged particles, and the same is true for the hadron multiplicities.

3.2 Multiplicities in gluon jets

The evolution equations (5) yield also results on the mean multiplicity $\mathcal{N}_g$ in gluon jets. The results derived here refer to the multiplicity in the full hemisphere of the gluon jet and can be measured, for example, in a final state with a primary gg colour singlet state. Such a state is expected to be produced in the decay of heavy quarkonia, recently the multiplicity in the decay $Y \to gg\gamma$ has been studied by the CLEO Collaboration [21]. An initial state of this type can also be realized approximately in $e^+e^- \to 3$ jets with nearly antiparallel q and $\overline{q}$ recoiling against the gluon [22] and this configuration has been analysed by the OPAL Collaboration [23]. Of special interest is the ratio of gluon and quark jet multiplicity $r = \mathcal{N}_g/\mathcal{N}_q$.

There are various results on r from $e^+e^- \to 3$ jets where the gluon is emitted from the quark with a smaller angle. In this case the radiation from the gluon jet around 90 degrees is suppressed and our results cannot be applied immediately; the observed excess of multiplicity ($r > 1$) is found consistent with QCD Monte Carlo calculations (for reviews, see [24,13]).

The ratio r approaches asymptotically the value $r = \frac{9}{4}$ [25]. The next-to-leading order corrections decrease this ratio at finite energies [26] and yet further with the inclusion of higher order corrections [27,28]. There is an uncertainty with this kind of asymptotic predictions in that the region of validity is not known a priori. A complete solution of the evolution equations (5) requires an initial value for the multiplicities. Such results with absolute normalization have been presented within the MLLA [9].

We have obtained the results from our evolution equation (5) with initial condition (11), however, we have not yet included a low energy correction term as in (14) which is beyond the scope of this paper. The results for the ratio r are shown in Fig. 2 again as function of $y_c = (Q_c/Q)^2$ for hadron multiplicities in comparison with the OPAL data from 3 jet events and the CLEO data on Y decays. Also shown is the prediction for jets at fixed $Q = 91$ GeV which could be tested using the same type of 3-jet data.

There is a very good agreement of our calculation with the OPAL data which refer to jet energies of $\sim$40 GeV. From Fig. 1b one may expect that the inclusion of the full $\mathcal{O}(\alpha_s)$ corrections would not modify the prediction essentially (by more than about 10%). On the other hand, the CLEO data fall considerably below the prediction $r \sim 1.25$ from the evolution equation. In this region, however, the low energy corrections may not be small: in Fig 1b these corrections correspond to a factor of two. A more precise prediction of the Y data will require the inclusion of the full $\mathcal{O}(\alpha_s)$ correction to the $Y \to gg\gamma$ process. In the low energy region where the configurations with large relative angles dominate the additional gluon could be produced from the heavy quark and not from the gluon, as naively expected; then the rate would be proportional to C_F and not to N_C resulting in a smaller value of r.

4 Conclusions

We solved the evolution equations for quark and gluon jets exactly by numerical integration and also supplemented the full $\mathcal{O}(\alpha_s)$ correction. With this improved accuracy we obtain a unified description with common absolute normalization of the mean jet multiplicity at LEP-1 and the hadron multiplicities in the energy range from 3 to 91 GeV within the errors or at least within 5%. In this description only the QCD scale Λ and a $k_\perp$ cutoff parameter $Q_0 \gtrsim \Lambda$ for the hadrons according to the LPHD picture have been adjusted to the data. The ratio of gluon to quark multiplicity at LEP-1 is described as well.

Of particular interest is the success of this model in the regions where perturbative QCD is not expected to be relevant a priori, namely for small transverse momenta, where the running coupling gets large, either for hadron multiplicities near threshold or for jet multiplicities of very high resolution. In both cases the strong effect of the running α_s is clearly seen from the comparison of the two multiplicities at the same scale y_c. It appears that perturbative QCD is still successful in these extreme kinematic regions for this inclusive quantity.

The model for hadron production emerging from this analysis is very simple. A hadron can be treated like a narrow parton jet but with the radiated partons being so soft ($\Lambda < k_\perp < Q_0$) that they cannot be resolved and are therefore confined in a region characterized by the hadronic scale Q_0 of a few hundred MeV. So the hadrons in this picture do not correspond to a colour singlet state of "valence partons" but rather to a parton (quark or gluon) with about the same momentum together with a "sea" of soft confined partons which take care of the colour neutralization. In this way the soft confinement picture can become consistent with the perturbative jet evolution.

It will be interesting to test this picture further by investigating the various predictions at different energies, especially in the transition region from jets to hadrons. Also the extension to other observables is feasible.

References

[1] D. Amati and G. Veneziano, Phys. Lett. **B83** (1979) 87;
A. Bassetto, M. Ciafaloni and G. Marchesini, Phys. Lett. **B83** (1979) 207;
G. Marchesini, L. Trentadue and G. Veneziano, Nucl. Phys. **B181** (1981) 335.

[2] Yu. L. Dokshitzer, D. I. Dyakonov and S. I. Troyan, Phys. Rep. **58** (1980) 270.

[3] Ya. I. Azimov, Yu. L. Dokshitzer, V. A. Khoze and S. I. Troyan, Z. Phys. **C27** (1985) 65 and **C31** (1986) 213.

[4] OPAL Collaboration: M. Z. Akrawy et al., Phys. Lett. **B247** (1990) 617.

[5] S. Lupia and W. Ochs, Phys. Lett. **B365** (1996) 339; preprint MPI-PhT/97-26 (hep-ph/9704319), "Low and High Energy Limits of Particle Spectra in QCD-jets", to appear in Z. Phys. C.

[6] G. Kramer and B. Lampe, Fortschr. Phys. **37** (1989) 161; Z. Phys. **C34** (1987) 497; Z. Phys. **C39** (1988).

[7] Report of the Hard QCD Working Group: W. J. Stirling, J. Phys. **G17** (1991) 1567.

[8] S. Catani, Yu. L. Dokshitzer, M. Olsson, G. Turnock and B. R. Webber, Phys. Lett. **B269** (1991) 432.

[9] S. Catani, Yu. L. Dokshitzer, F. Fiorani and B. R. Webber, Nucl. Phys. **B377** (1992) 445.

[10] Yu. L. Dokshitzer and M. Olsson, Nucl. Phys. **B396** (1993) 137.

[11] L3 Collaboration: O. Adriani et al., Phys. Lett. **B284** (1992) 471.

[12] OPAL Collaboration: R. Acton et al., Z. Phys. **C59** (1993) 1.

[13] V.A. Khoze and W. Ochs, "Perturbative QCD approach to multiparticle production", preprint DTP/96/36, MPI-PhT-96/29 (hep-ph/9701421), Int. J. Mod. Phys. A in press.

[14] Yu. L. Dokshitzer and S. I. Troyan, Proc. 19th Winter School of the LNPI, Vol. 1, p.144; Leningrad preprint LNPI-922 (1984).

[15] Yu. L. Dokshitzer, V. A. Khoze, A. H. Mueller and S. I. Troyan, Rev. Mod. Phys. **60** (1988) 373; "Basics of Perturbative QCD", ed. J. Tran Thanh Van, Editions Frontiéres, Gif-sur-Yvette, 1991.

[16] B. I. Ermolayev and V. S. Fadin, JETP. Lett. **33** (1981) 285;
A. H. Mueller, Phys. Lett. **104B** (1981) 161.

[17] Yu. L. Dokshitzer, Sov. Phys. JETP, **46** (1977) 641;
G. Altarelli and G. Parisi, Nucl. Phys. **B126** (1977) 298.

[18] Yu. L. Dokshitzer, V. A. Khoze and S. I. Troyan, Int. J. Mod. Phys. **A7** (1992) 1875.

[19] N. Brown and W. J. Stirling, Phys. Lett. **B252** (1990) 657; Z. Phys. **C53** (1992) 629.

[20] MARK I Coll., J. L. Siegrist et al., Phys. Rev. **D26** (1982) 969;
JADE Coll., W. Bartel et al., Z. Phys. **C20** (1983) 187;
PLUTO Coll., C. Berger et al., Phys. Lett. **B95** (1980) 313;
TASSO Coll., W. Braunschweig et al., Z. Phys. **C45** (1989) 193;
TPC/2γ Collaboration: H. Aihara et al., Phys. Lett. **B134** (1987) 299;
HRS Coll., M. Derrick et al., Phys. Rev. **D34** (1986) 3304;
TOPAZ Coll., M. Yamauchi et al., Proc. XXIV Int. Conf. on High Energy Physics (Munich, 1988), Springer Verlag, Eds. R. Kotthaus and J. H. Kühn, p. 852;
AMY Coll., H. W. Zheng et al., Phys. Rev. **D42** (1990) 737;
ALEPH Coll., D. Decamp et al., Phys. Lett. **B273** (1991) 181;
DELPHI Coll., P. Abreu et al., Z. Phys. **C50** (1991) 185;
OPAL Coll., D. Acton et al., Z. Phys. **C53** (1992) 539;
L3 Coll., B. Adeva et al., Z. Phys. **C55** (1992) 39;
MARKII Coll., G. S. Abrams et al., Phys. Rev. Lett. **64** (1990) 1334.

[21] CLEO Coll., M. S. Alam et al., Phys. Rev. **D56** (1997) 17.

[22] J. W. Gary, Phys. Rev. **D49** (1994) 4503.

[23] OPAL Coll., G. Alexander et al., Phys. Lett. **B388** (1996) 659.

[24] J. Fuster, S. Cabrera and S. Marti i Garcia, Nucl Phys. **B54A** (Proc. Suppl.) (1997) 39.

[25] S. J. Brodsky and J. F. Gunion, Phys. Rev. Lett. **37** (1976) 402.

[26] A. H. Mueller, Nucl Phys. **B241** (1984) 141;
E. D. Malaza, B. R. Webber, Phys. Lett. **B149** (1984) 501; Nucl. Phys. **B267** (1986) 70.

[27] J. B. Gaffney and A. H. Mueller, Nucl. Phys. **B250** (1985) 109.

[28] I. M. Dremin and V. A. Nechitailo, Mod. Phys. Lett. **A9** (1994) 1471;
I. M. Dremin and R. C. Hwa, Phys. Lett. **B324** (1994) 477.

Figure Captions

Fig. 1a: Data on the average jet multiplicity at $Q = 91$ GeV[11,12] and the average particle multiplicity (assuming $\mathcal{N} = \frac{3}{2}\mathcal{N}_{ch}$) at different *cms* energies[20] with $Q_c = 0.507$ GeV as a function of y_c. The solid (dashed) line shows the prediction in absolute normalization for the particle (jet) multiplicity obtained by using eq. (14) with parameters from eq. (16).

Fig. 1b: Data as in Fig. **1a**, but $\mathcal{N} - 2$ is now shown. The solid lines show the complete predictions of eq. (14) for both the particle and jet multiplicities, the dashed lines the contribution for eq. (5) alone. The same parameters as in Fig. **1a** are used.

Fig. 2: Data on the ratio of average particle multiplicities in quark and gluon jets[21,23] with $Q_c = 0.507$ GeV as a function of y_c. The solid (dashed) line shows the prediction for the ratios of particle (jet) multiplicities in quark and gluon jets obtained by using eq. (5) with the same parameters as in Fig. **1**.

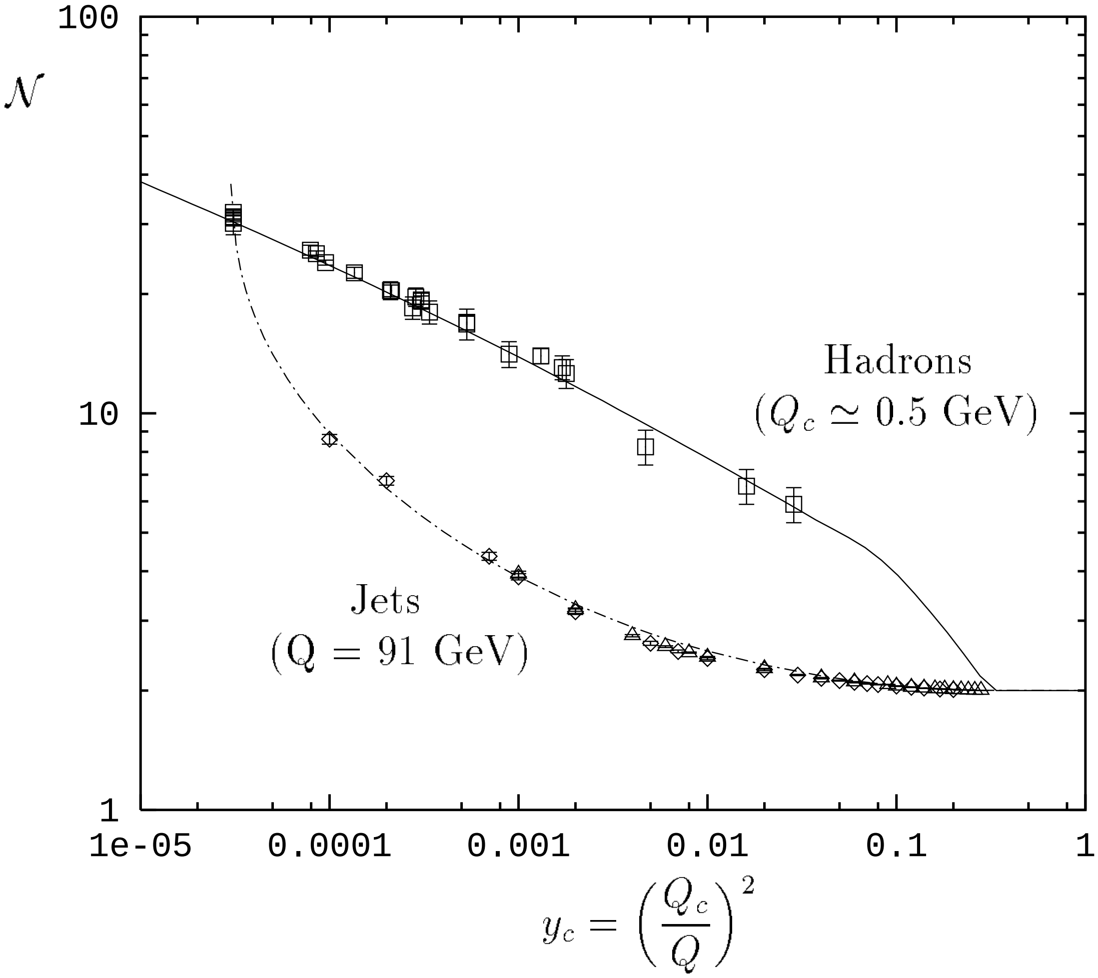

100
$\mathcal{N}$
10
1
1e-05
0.0001
0.001
0.01
0.1
1
Hadrons
($Q_c \simeq 0.5$ GeV)
Jets
(Q = 91 GeV)
$y_c = \left(\frac{Q_c}{Q}\right)^2$

Figure 1: a

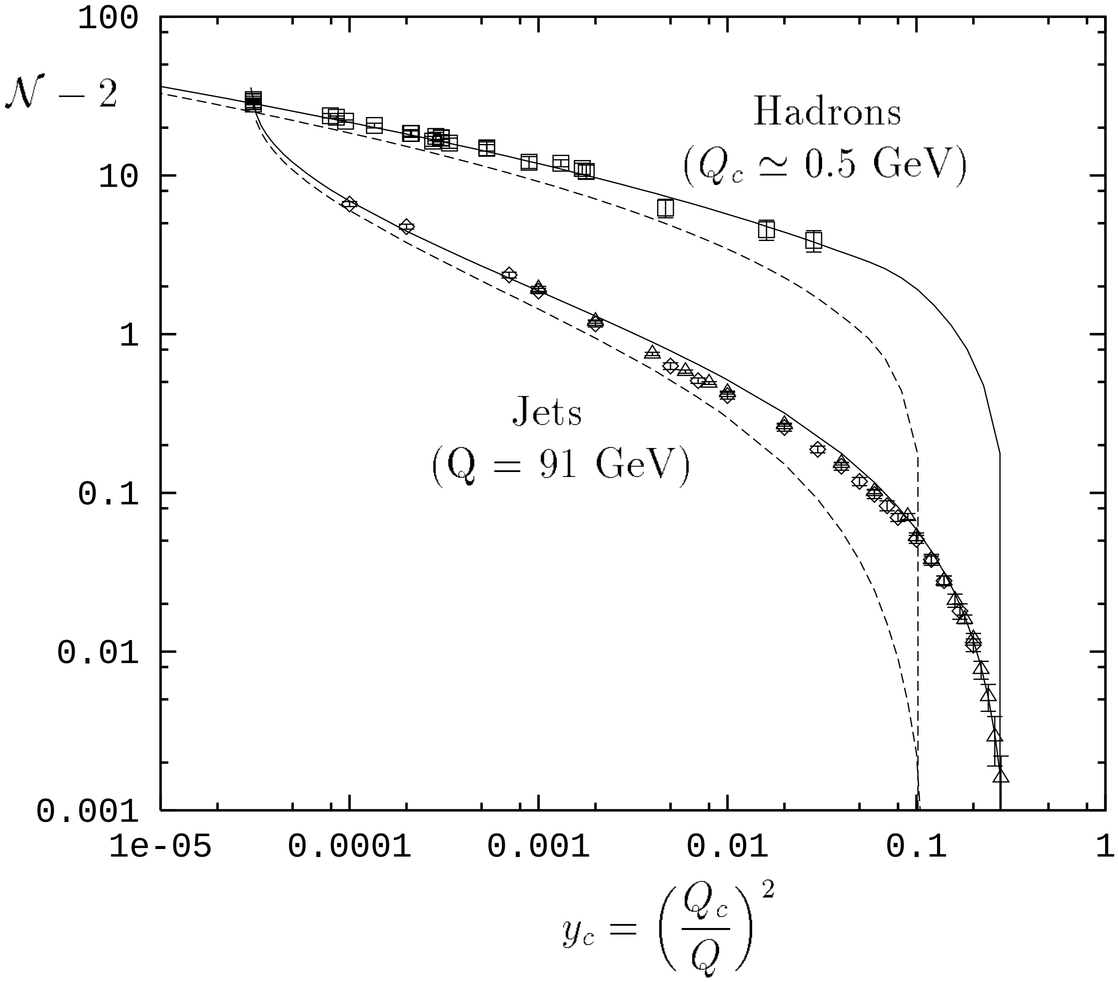
100
10
1
0.1
0.01
0.001
$\mathcal{N}-2$
Hadrons
($Q_c \simeq 0.5$ GeV)
Jets
(Q = 91 GeV)
1e-05
0.0001
0.001
0.01
0.1
1
$y_c = \left(\frac{Q_c}{Q}\right)^2$

Figure 1: b

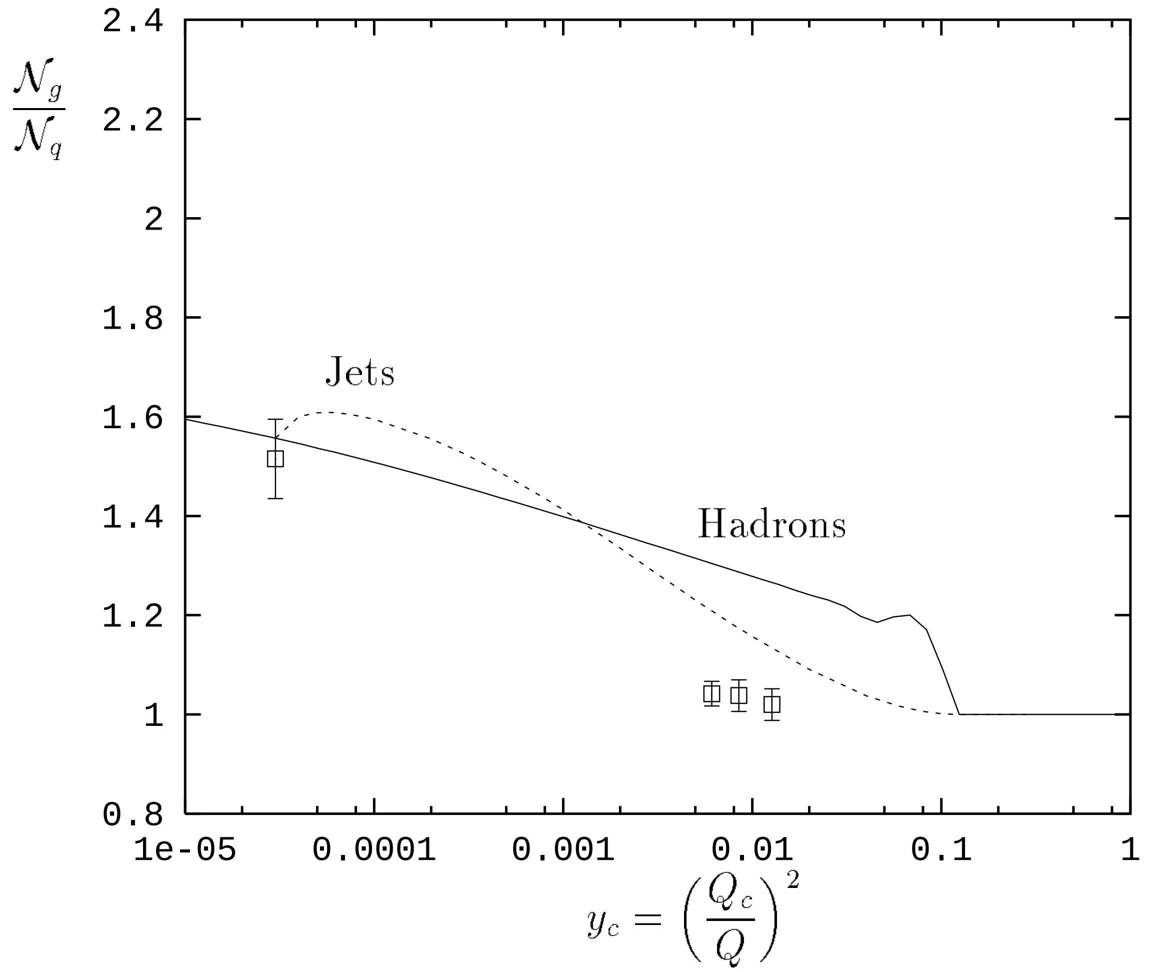

$\frac{\mathcal{N}_g}{\mathcal{N}_q}$
2.4
2.2
2
1.8
1.6
1.4
1.2
1
0.8
1e-05
0.0001
0.001
0.01
0.1
1
Jets
Hadrons
$y_c = \left(\frac{Q_c}{Q}\right)^2$

Figure 2: